Wetting-induced depletion interaction between particles in a phase-separating liquid mixture

Takeaki Araki and Hajime Tanaka
Institute of Industrial Science, University of Tokyo, Meguro-ku, Tokyo 153-8505, Japan
(Received 20 December 2005; revised manuscript received 17 February 2006; published 19 June 2006)

Inclusion of solid particles drastically affects the pattern evolution of phase separation of a binary fluid mixture, via preferential wetting of one of the phases to the particles. Here we study this problem by numerical simulation, which incorporates interparticle hydrodynamic interactions properly. When particles favor one of the components of a mixture, wetting layers are quickly formed on the particle surfaces and all particles are eventually included into the more wettable phase. For immobile particles, domains of the more wettable phase are pinned to the particles and the domain growth is thus suppressed. For this case, the domain size at a certain phase-separation time decreases monotonically with increasing the particle concentration. For mobile particles, on the other hand, the reentrant morphological transformation is observed as a function of the particle concentration: With an increase in the particle concentration, the domain morphology of the more wettable phase sequentially changes from network, droplet to network. We found that the final morphological transition is induced by wetting-induced depletion interaction: Strong attractive interactions act among particles when the total volume of the more wettable phase is not enough to cover all the particles by wetting layers.

DOI: 10.1103/PhysRevE.73.061506 PACS number(s): 64.75.+g, 68.08.Bc, 81.07.−b, 82.20.Wt

I. INTRODUCTION

Wetting phenomena [1,2] are known to drastically affect phase separation and the resulting pattern evolution [3]. For a binary mixture containing particles, particles induce complex dynamic couplings between wetting and phase separation due to their mobility and produce a rich variety of morphology [4,5]. Usually particles favor one of the phases, which is the situation we consider here, although neutral particles can sit just on the domain interface [6,7]. Upon phase separation, wetting layers are quickly formed on the particle surfaces [8] and then phase separation proceeds so that the phase more wettable to particles contains all the particles. This problem has been intensively studied both experimentally [4,9,10] and numerically [11–22]. To understand the pattern evolution kinetics, the hydrodynamic interaction between particles is one of the most difficult but important problems. A few numerical methods have been employed, which include a cell dynamics method [15], a lattice Boltzmann method [16,17], a molecular dynamics method [18,19], and a dissipative particle dynamics method [20]. These studies revealed that the introduction of particles into a binary fluid mixture suppresses the hydrodynamic flow induced by the interface motion and thus the domain growth slows down [15–18].

Here we propose a numerical method based on a "fluid particle dynamics (FPD)" method [23] to incorporate effects of phase separation and wetting together with hydrodynamic effects. In our FPD method we solve flow in a system by using a continuous field variable, and we can thus easily incorporate various continuous field variables (order parameters) into a host fluid. In other words, we can use our FPD scheme for colloidal particles immersed in various complex fluids such as an electrolyte [24], a nematic liquid crystal [25], and a binary fluid mixture (this study). This is one of the remarkable merits of this method. Here we incorporate compositional order parameter to a host fluid. Then, we study the kinetics of pattern evolution of a phase-separating binary liquid mixture containing particles by using the above method. In particular, we investigate effects of the mobility of particles. We report an unconventional interparticle interaction mediated by wetting layers on the particle surfaces and the resulting reentrant morphological transition as a function of the particle concentration.

The organization of this paper is as follows. In Sec. II we explain how to extend our FPD method for a wetting problem. In Sec. III we show simulation results. In Sec. IV we discuss interparticle interactions induced by wetting effects. In Sec. V we summarize our paper.

II. NUMERICAL SIMULATION METHOD

A. Extension of the FPD method for a wetting problem

First we explain our simulation method. The coarse-grained variables relevant for the physical description of phase-separation dynamics of a fluid mixture containing particles are a particle position $\{\mathbf{r}_i\}$, a concentration field ψ, and a fluid velocity field $\boldsymbol{v}$. Index i stands for an individual particle. We describe fluid particle i using a hyperbolic tangent function as

$$\phi_i(\mathbf{r}) = [\tanh\{(a - |\mathbf{r} - \mathbf{r}_i|)/d\} + 1]/2, \tag{1}$$

where a and d are the radius and interface width of a particle, respectively [23]. We employ the following free energy functional for a binary mixture containing particles:

$$\mathcal{F}\{\psi,\phi\} = \int d\mathbf{r}\left\{ f(\psi) + \frac{K}{2}|\nabla\psi|^2 + Wd\psi|\nabla\phi|^2 + \chi(\psi - \bar{\psi})^2\phi \right\}. \tag{2}$$

The first and second terms of the right-hand side (r.h.s.) of Eq. (2) correspond to the Ginzburg-Landau type mixing free energy of a binary mixture with

$$f(\psi) = -\frac{\tau}{2}\psi^2 + \frac{u}{4}\psi^4, \tag{3}$$

where τ, u, and K are positive constants. The third one stands for the wetting interaction between a binary mixture and a particle surface (represented as $|\nabla\phi|^2$ in our scheme). W represents the strength of this wetting interaction; here $W<0$ means that the phase of $\psi>0$ favors a particle surface. Hereafter, we denote the phase more wettable to particles as "A," and the other as "B." The fourth term is introduced so that the concentration field inside each particle becomes $\psi \approx \bar{\psi}$ ($\bar{\psi}$ being the average concentration), where $\chi(>0)$ is its coupling constant.

The time development of the concentration and velocity fields are described by

$$\frac{\partial\psi}{\partial t} = -\boldsymbol{v}\cdot\nabla\psi + L\nabla^2\mu + \theta, \tag{4}$$

$$\rho\frac{\partial\boldsymbol{v}}{\partial t} = \mathbf{F} - \psi\nabla\mu - \nabla p + \nabla\cdot[\eta\{\nabla\boldsymbol{v} + (\nabla\boldsymbol{v})^T\}], \tag{5}$$

where μ is the chemical potential defined as $\mu = \frac{\delta}{\delta\psi}\mathcal{F}$. θ represents the thermal fluctuation of the composition. L and ρ are, respectively, the diffusion constant and the density, both of which are assumed to be independent of ψ. η is the space-dependent viscosity, which represents the particle distribution in our FPD scheme [23]

$$\eta(\mathbf{r}) = \bar{\eta} + \Delta\eta\sum_i \phi_i(\mathbf{r}). \tag{6}$$

The first term of r.h.s. of Eq. (5) is the force field stemming from particles:

$$\mathbf{F}(\mathbf{r}) = \sum_i \mathbf{F}_i\phi_i(\mathbf{r})/A_i. \tag{7}$$

Here $\mathbf{F}_i$ is the force acting on particle i, which is given by

$$\mathbf{F}_i = -\frac{\partial}{\partial\mathbf{r}_i}\sum_{j\neq i} V(|\mathbf{r}_i - \mathbf{r}_j|) - \zeta\frac{d}{dt}\mathbf{r}_i, \tag{8}$$

and A_i is the area [or volume in three-dimensional (3D)] of an individual particle i: $A_i = \int d\mathbf{r}\,\phi_i(\mathbf{r})$.

We employ the repulsive part of the Lennard-Jones potential as a direct interparticle interaction

$$V(r) = 4\epsilon\left\{\left(\frac{2a}{r}\right)^{12} - \left(\frac{2a}{r}\right)^{6} + \frac{1}{4}\right\} \text{ for } r < 2^{7/6}a,$$

$$V(r) = 0 \text{ for } r > 2^{7/6}a.$$

In the above, ζ is the frictional coefficient for the particle motion, which is introduced to control the mobility of particles (see below). Here we emphasize that ζ is nothing to do with the fluid viscosity.

The second term of r.h.s. of Eq. (5) represents the force stemming from the osmotic pressure [26]. p is a part of pressure, which is imposed to satisfy the incompressible condition $\nabla\cdot\boldsymbol{v}=0$. The motion of particle i is given by the averaged velocity field inside the particle as [23]

$$\frac{d\mathbf{r}_i}{dt} = \frac{\int d\mathbf{r}'\,\boldsymbol{v}(\mathbf{r}')\phi_i(\mathbf{r}')}{A_i}. \tag{9}$$

B. Details of our simulation

1. On the dimensionality of simulation

In this paper, we make a two-dimensional (2D) simulation to save a computational cost, although our method itself can be applied to a 3D system straightforwardly. Here we make a few comments on this dimensionality problem. Our 2D simulation may be relevant to a phase-separating Langmuir film with colloidal particles, or a phase-separating membrane including proteins, although it is less obvious how to introduce ζ experimentally in these examples. Our simulation may also capture some features observed in our quasi-2D experiments, in which we used sandwiched cells with glass plates [4,5]. In these experiments, the friction arises from contacts of particles to the sample cell walls such that it can be controlled by changing the ratio of sample thickness and particle size.

2. Parameter setting

In this study we set the correlation length of critical concentration fluctuations to be the interfacial width of a particle: $d=\sqrt{K/\tau}$. Hereafter we scale the length and time by d and the characteristic lifetime of critical fluctuations, d^2/L, respectively. In the following simulations, we set the parameters as $\tau=1$, $u=1$, $K=1$, and $L=1$. We solve the above kinetic equations by the explicit Euler scheme using the lattice space $\Delta x=1$ and the time increment $\Delta t=0.01$ in a 2D space. The system size was 256×256. We constantly impose Gaussian thermal fluctuation of the concentration, whose intensity is $|\theta|=10^{-4}$. Equation (5) is solved by the Makers and Cell (MAC) method with a staggered lattice. To get rid of the inertia effect (Stokes approximation), we iterate the calculation of Eq. (5) to satisfy $|\rho\frac{\partial}{\partial t}\boldsymbol{v}| < 10^{-2}|\mathbf{F} - \psi\nabla\mu|$. Viscosity parameters are set as $\bar{\eta}=0.5$ and $\Delta\eta=24.5$, which mean that the viscosity ratio between the inner and outer parts of a particle is 50.

The other parameters are set as $a=2$, $d=1$, $\epsilon=1$, $\chi=2$, and $W=-8$. With these parameters, phase A covers the particle surface completely. Because the particles are rather small and the concentration of phase A increases around a particle, we confirm that the volume fraction of phase A containing particles is almost independent of the particle number N_p for these parameters. That is, the volumes of the two separating phases are the same for any N_p: The "volume symmetry" is preserved. This allows us to study solely effects of the concentration and the mobility of particles, free from the volume-symmetry effect on the phase-separation morphology.

III. RESULTS

A. Phase separation of fluid mixtures containing immobile particles

First we show results for a symmetric liquid mixture ($\bar{\psi}=0.0$) containing immobile particles in Fig. 1. We used ζ

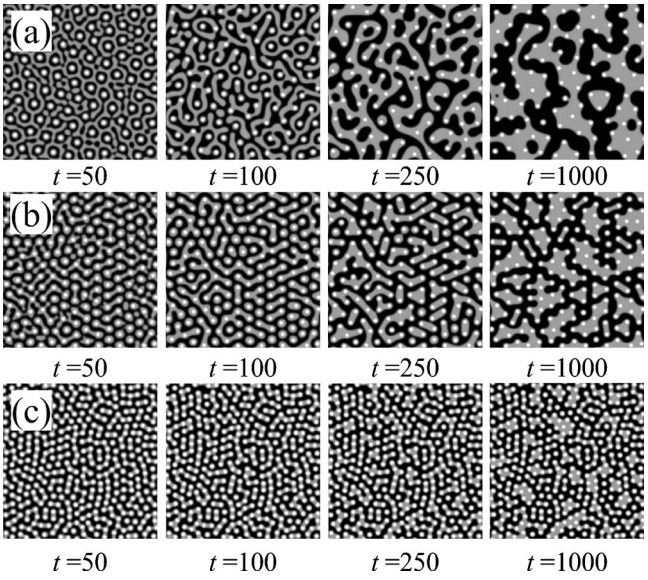

FIG. 1. Pattern evolution of a symmetric liquid mixture containing immobile particles (white circles) (ζ=200): (a) N_p=100, (b) N_p=196, and (c) N_p=400. The brightness of the matrix liquid represents the concentration field ψ: Gray and black color represent phases A and B, respectively. The size of particles are enlarged by a factor of 2 to make them visible.

=200 to make particles immobile. For this ζ, we confirmed that particles do not move during the simulation period. In the early stage of phase separation, spinodal decomposition induces concentric target patterns around particles due to wetting effects [9,22]: Phase A covers a particle surface, which induces a depleted region around it as a result of diffusion (see, e.g., Fig. 7). Then the remaining mixture phase separates and the surface-wetting layers around particles are bridged. The domains grow with time to reduce the interface energy, but very slowly since they are pinned to the immobile particles. The hydrodynamic coarsening mechanism and the Brownian-coagulation mechanism cannot operate once the domain interface is pinned; thus, diffusion is the only process of material transport after pinning [4,5]. In the late stage ($t>250$), most particles are located on the domain interface. This is a consequence of the interface pinning by particles. For larger N_p, domains are pinned in the earlier stage and thus the domain size becomes smaller.

Figure 2(a) shows the time development of the structure factor of a symmetric mixture containing immobile particles (N_p=400) [see Fig. 1(c)]. The structure factor is calculated as

$$S(q) = \frac{1}{2\pi q \Delta q} \int_{q \leqslant |\mathbf{q}'| \leqslant q+\Delta q} d\mathbf{q}' \langle \tilde{\psi}(\mathbf{q}') \tilde{\psi}(-\mathbf{q}') \rangle, \quad (10)$$

where $\tilde{\psi}(\mathbf{q})$ is the Fourier transform of $\psi(\mathbf{r})$. The time development of the structure factor does not obey a dynamic scaling law. In Fig. 2(a), the structure factor has a fixed peak around $q \sim 0.5$, which reflects the spatial correlation in particle positions. The small peaks and shoulders in $q>0.5$ are from the particle form factor. Although there is no significant change in the structure factor for $q>0.5$, the intensity grows

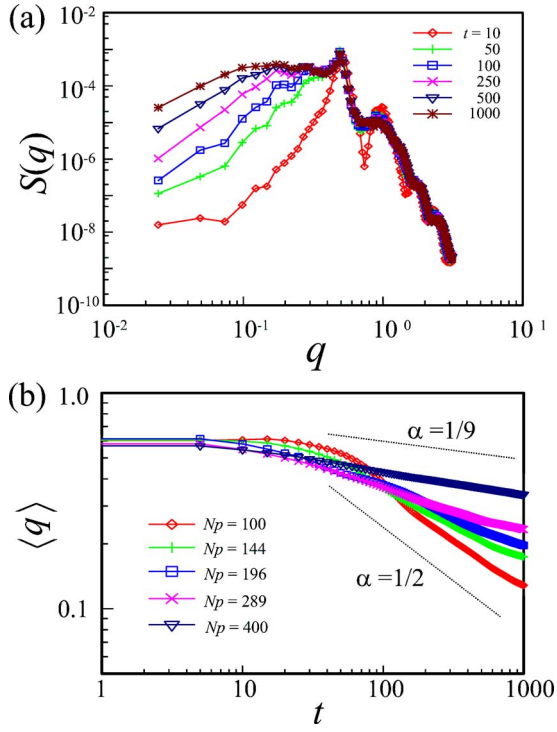

FIG. 2. (Color online) (a) Time development of $S(q)$ of a symmetric fluid mixture including N_p=400 immobile particles (ζ^{-1}=0.005)[see Fig. 1(c)]. (b) Temporal change of the characteristic wave number $\langle q \rangle$ for mixtures including fixed particles.

with time for $q<0.5$. This indicates that only the part of phase A bridging fixed particles coarsens with time.

Figure 2(b) represents the temporal evolution of the characteristic wave number of $S(q)$ for various N_p. The characteristic wave number is calculated as

$$\langle q \rangle = \int dq\, qS(q) \Big/ \int dq\, S(q). \quad (11)$$

We can see in Fig. 2(b) that the domain growth slows down in the late stage ($t>100$) for larger N_p. $\langle q \rangle$ decays with time apparently obeying the following power law: $\langle q \rangle \propto t^{-\alpha}$. Here α depends on the particle number N_p. For N_p=400, $\alpha \sim 1/9$, which indicates that the presence of fixed particles not only suppresses hydrodynamic coarsening, but also diffusional one. We note that the local curvature of the domain interface is not directly correlated with the domain size, but rather with N_p. Thus, the Lifshitz-Slyozov mechanism does not operate efficiently, which explains why the coarsening is so slow [4,5]. In the early stage, $\langle q \rangle$ is smaller for larger N_p. This is because the phase separation is accelerated around particles by wetting effects.

B. Phase separation of fluid mixtures containing mobile particles

Figure 3 shows results for a symmetric mixture containing mobile particles (ζ=2). The behavior in the early stage is essentially the same as that for the above immobile particle cases. Since particles are mobile, however, domains keep

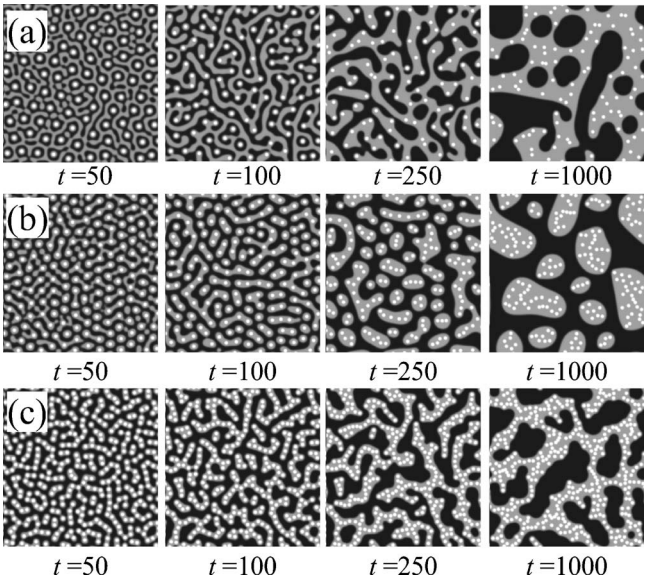

FIG. 3. Pattern evolution of a symmetric liquid mixture containing mobile particles ($\zeta=2$). (a) $N_p=100$, (b) $N_p=196$, and (c) $N_p=400$. The brightness of the matrix liquid represents the concentration field ψ: Gray and black color represent phases A and B, respectively. The size of particles are enlarged by a factor of 2 to make them visible.

growing even in the late stage unlike the immobile particle case. We found an interesting reentrant morphological change of the late-stage domain pattern as a function of N_p. Without particles, a symmetric pattern is formed due to the volume symmetry [26]. For $N_p=100$, the morphological symmetry is broken and phase B forms droplets [see Fig. 3(a)]. For $N_p=196$, on the other hand, phase A forms droplets [see Fig. 3(b)]. For $N_p=400$, phase A forms a networklike structure [see Fig. 3(c)]. As noted before, the volume fraction of phase A including particles does not depend on N_p. Thus, this unusual morphological change is not induced by the change of the volume symmetry between the two phases.

Figure 4(a) shows the time development of $S(q)$ for a mixture including mobile particles ($N_p=400$) [see Fig. 3(c)]. Contrary to the immobile particle case [see Fig. 2(a)], the peak position shifts to lower q with time. The dynamics of the pattern evolution is very different from that in a mixture including no particle [in particular, see Fig. 3(c)]. Figure 4(b) shows the temporal evolution of the characteristic wave number of $S(q)$ for several N_p. In the early stage ($t<200$), the domain growth is faster for larger N_p, as can also be seen in Fig. 3. $\langle q\rangle$ decreases faster than in immobile particle cases for all N_p. Save for $N_p=400$, the late-stage growth dynamics is almost independent of N_p. The exponent of the power-law growth is $\alpha\sim 1/2$, which seems to be consistent with that of a symmetric fluid mixture in 2D [27].

As shown in Fig. 3, the pattern evolution of mixtures including mobile particles has interesting character, which cannot be explained by the knowledge on normal phase separation of a binary fluid mixture without particles. Since the Fourier-space analysis does not provide useful information on the morphological characteristics of the domain pattern, we will study this point in a real-space morphological analysis.

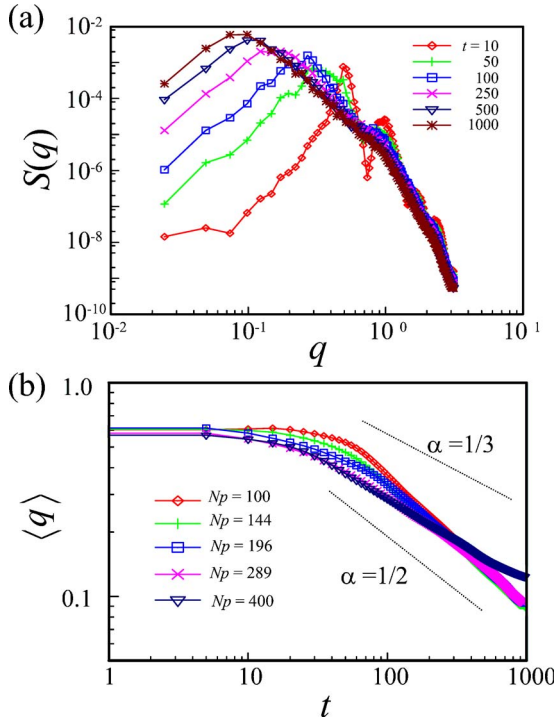

FIG. 4. (Color online) (a) Time development of $S(q)$ for a symmetric fluid mixture including $N_p=400$ mobile particles ($\zeta^{-1}=0.5$) [see Fig. 3(c)]. (b) Temporal change of the characteristic wave number $\langle q\rangle$ for mixtures including mobile particles.

C. Characterization of domain morphology

Figure 5 summarizes the dependences of the simulated domain pattern at $t=1000$ on N_p and ζ^{-1}. We can see reentrant morphological changes of the domain pattern as a function of N_p and ζ^{-1}. The time development of the structure factor provides useful information if the topology of the domain pattern is well characterized beforehand. However, it is not so useful for the characterization of domain topology itself. Thus we use the 2D Minkovski functional [28], which

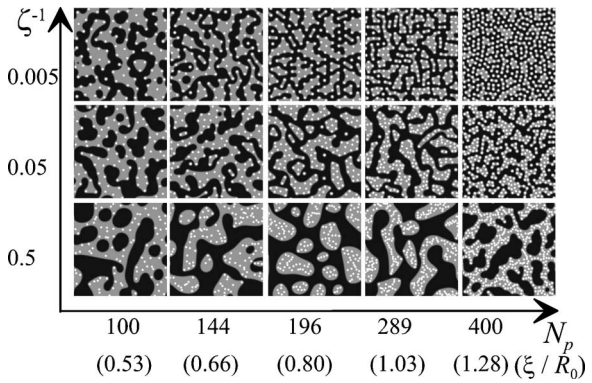

FIG. 5. Dependences of the domain pattern at $t=1000$ on the particle number N_p (or ξ/R_0; on its definition see Sec. IV B) and the mobility ζ^{-1}. The brightness of the matrix liquid represents the concentration field ψ: Gray and black color represent phases A and B, respectively. The size of particles are enlarged by a factor of 2 to make them visible.

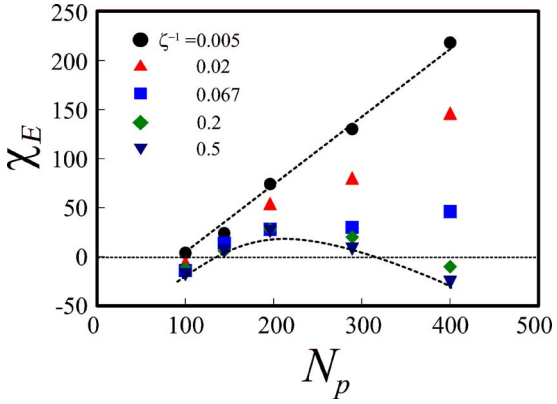

FIG. 6. (Color online) N_p dependence of the 2D Minkovski functional χ_E at $t=1000$ for particles with different mobility.

corresponds to the Euler characteristic in 3D. Here we briefly explain how to calculate the 2D Minkovski functional. First we label a lattice site with $\psi>0$ as A and a lattice site with $\psi<0$ as B. F_L is the number of lattice sites A. V_o is the number of vertices that have A sites as neighbors, but are not fully surrounded by A sites. V_i is the number of vertices that are completely surrounded by four A sites. E_i is the number of edges between two neighboring A sites and E_o is the number of edges between A and B sites. Using these values, the 2D Minkovski functional χ_E is calculated as $\chi_E=2F_L+V_o+2V_i-E_o-2E_i$. In our definition, the positive value of χ_E means that phase A forms droplets and $\chi_E/2$ corresponds to the number of phase A droplets.

Figure 6 shows results of our analysis of the 2D Minkovski functional. For immobile particles ($\zeta=200$), χ_E is always positive and monotonically increases with increasing N_p: Phase A always forms a droplet structure and the domain size is smaller for larger N_p, consistent with what we see in Fig. 1. For the same N_p, χ_E decreases with decreasing ζ, which indicates that the number of droplets of phase A decreases with decreasing ζ. This is because the mobility of droplets containing particles decreases for larger ζ, which suppresses the Brownian coagulation and hydrodynamic coarsening mechanisms. For the most mobile particles ($\zeta=2$), χ_E becomes negative for both low ($N_p=100$) and high ($N_p=400$) particle concentration, whereas it is positive for $N_p=144$, 196, and 289. This is consistent with the fact that phase A forms a network structure for $N_p=100$ and $N_p=400$, whereas it forms a droplet structure for $N_p=196$ (see Fig. 3).

IV. DISCUSSION

A. Effects of wetting on interaction between two particles

Figure 7 shows the formation process of target patterns around two particles. The initial values of the compositional order parameter are $\bar{\psi}=0.4$, 0.0, and −0.4 for Figs. 7(a)–7(c), respectively. The corresponding volume fractions of phase A are 70, 50, and 30 %. After the formation of target patterns the particles approach with each other (see also Fig. 8), which indicates there exists an attractive interaction between

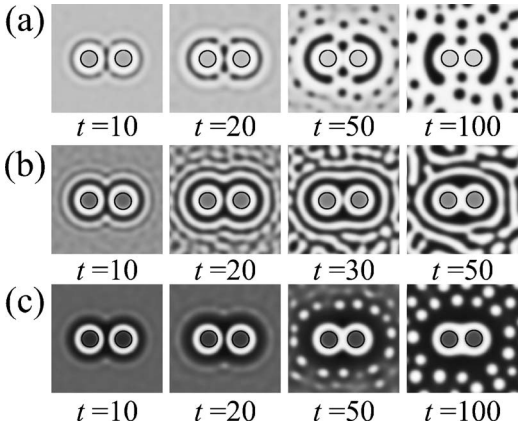

FIG. 7. A process of target pattern formation around two particles (black circles) immersed in a mixture and the resulting motion of the particles. The particle radius is $a=8$ and the initial separation is $\Delta r=24$. The initial values of the compositional order parameter are $\bar{\psi}=-0.4$ (a), 0.0 (b), and 0.4 (c). Here the particles are drawn as their actual size.

the particles. Even in asymmetric mixtures, the concentric patterns are formed around the particles, which are selectively covered by phase A, as expected [9,22]. Subsequently the depleted regions are formed around the covered particles as a result of diffusional transport of phase A to the particle surfaces. Particles also approach with each other. In the far field, a dot pattern is formed as a result of the composition oscillation induced by wetting and the volume asymmetry. We can see the long-range nature of the wetting effects, which stems from the conserved nature of the composition order parameter.

Figure 8 shows the temporal change in the separation between attracting particles (see Fig. 7), in which the volume fraction of phase A is changed. The results show that this wetting-induced attractive interaction depends upon the particle number density and the interaction is switched on only after wetting layers are formed around the particles by phase separation. The attractive interaction is stronger for smaller $\bar{\psi}$, namely, with an increase in the degree of the lack of phase

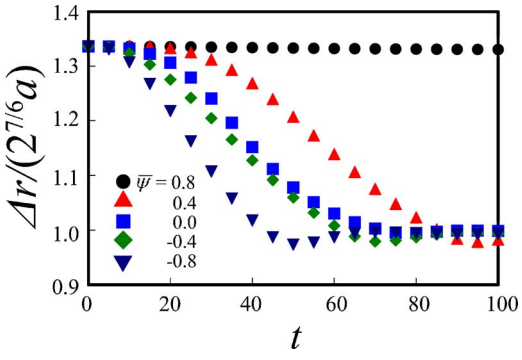

FIG. 8. (Color online) Temporal change of the separation between particles, which are interacting by a capillary force. Initially we put two particles in a mixture and measure the separation between the particles after the initiation of phase separation. The vertical axis is scaled by the diameter of the Lennard-Jones interaction.

A. In the mixture of $\bar{\psi}=0.8$, the amount of phase A is enough to completely cover the particles and thus there is no attraction. We call this unconventional attractive interaction between particles, "wetting-induced depletion attraction."

B. Mechanism of the interparticle attractive interaction: Wetting-induced depletion effects

Here we propose a mechanism responsible for this unusual reentrant morphological change. We introduce two key lengths characterizing a mixture containing particles: One is the thickness of the wettable layer (the first rim of a target pattern) of phase A initially formed around a particle ξ and the other is the average thickness of phase A around a particle at equilibrium R_0. As mentioned before, the target pattern is a result of surface-directed spinodal decomposition [8]. Thus, its characteristic length is given by the correlation length, i.e., the characteristic length of the most unstable mode of spinodal decomposition [22]

$$\xi \approx \pi\sqrt{2K/(\tau - 3u\bar{\psi}^2)}. \tag{12}$$

On the other hand, R_0 is straightforwardly calculated by a geometrical relation in 2D between the particle number density n_p and the volume fraction of phase A, $\Psi_0=(1+\bar{\psi})/2$, as

$$R_0 = [(\Psi_0 + \pi a^2 n_p)/(\pi n_p)]^{1/2} - a. \tag{13}$$

There can be the following three cases in terms of the relation between ξ and R_0: (i) $\xi < R_0$; (ii) $\xi \sim R_0$; and (iii) $\xi > R_0$. Case (i) corresponds to a case of a low particle number density. For this case, particles do not affect phase separation so strongly. In other words, a bicontinuous pattern is formed as in a symmetric mixture containing no particles. It is well known that the inclusion of particles increases the viscosity of the host liquid. In a symmetric mixture of two liquids having different viscosities, the more viscous phase tends to form a continuous structure due to the asymmetric stress division between the two phases [29]. Thus, phase A, whose viscosity effectively increases due to the particle inclusion, tends to form a continuous network structure in this case. This is consistent with what is seen in Fig. 3(a). For case (ii), phase A can be equally divided by each particle, and thus particles can be just covered by the wetting layer of thickness ξ. In this case, droplets of phase A are formed since it is a configuration suitable for covering particles by phase A. In general, the hydrodynamic coalescence of contacting droplets is faster than the collision interval determined by droplet diffusion by the Brownian motion. Thus, once the droplet pattern is formed, it grows with keeping this morphology [30]. Case (iii) corresponds to a case of a high particle density. In this case, phase A is not enough to wet particles. This means that the wetting layers have to be shared by more than two particles. Thus, this depletion of phase A leads to attractive interaction among particles. With a help of interparticle hydrodynamic interaction [23], the attractive interaction leads to the formation of a network structure [31], as shown in Fig. 3(c).

This mechanism of interparticle attraction in a phase-separating mixture has a connection to (a) wetting-induced interparticle interaction known for the one-phase region [32] and (b) a capillary force [1,33] which is induced by surface tension associated with a liquid bridging particles. However, our mechanism differs from these known ones in its dynamic character unique to the intrinsically nonequilibrium nature of phase separation, unlike the latter.

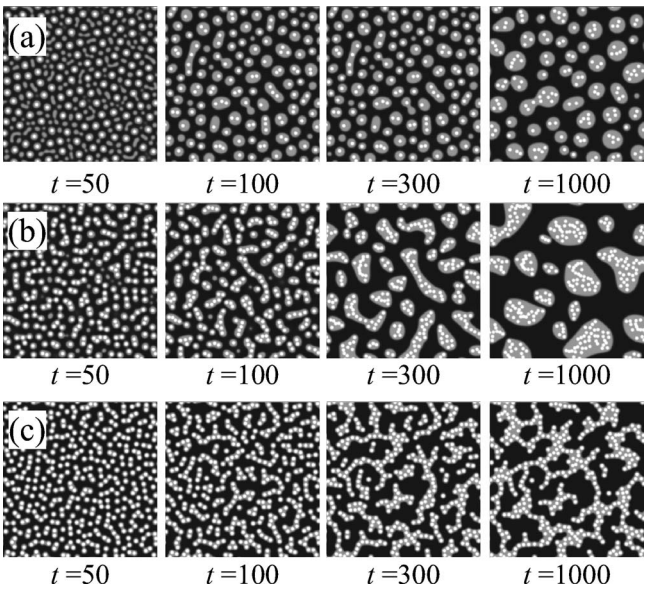

FIG. 9. Pattern evolution of an asymmetric liquid mixture ($\bar{\psi}=-0.2$) containing mobile particles (white circles) ($\zeta=2$): (a) $N_p=144$ ($\xi/R_0=0.81$), (b) $N_p=289$ ($\xi/R_0=1.27$), and (c) $N_p=400$ ($\xi/R_0=1.59$). The brightness of the matrix liquid represents the concentration field ψ: Gray and black color represent phases A and B, respectively. The size of particles are enlarged by a factor of 2 to make them visible.

C. Relevance of our mechanism

Finally we briefly discuss a problem associated with the dimensionality of our system (2D). In 2D it is known that any infinitesimal perturbation leads to the breakdown of the morphological symmetry. For example, imperfect compensation of the volume of phase A may cause such symmetry breaking. However, we believe that this is not the dominant mechanism and the behavior is really induced by wetting-induced depletion attraction. Figure 9 shows the morphological evolution for asymmetric mixtures of three particle densities. With an increase in N_p, i.e., ξ/R_0, the phase-separation morphology changes from a droplet to a network structure. The faster growth of droplets for (b) than (a) may be due to the stronger attractive interaction between particles, reflecting larger ξ/R_0. Note that for $\xi/R_0 \leqslant 0.8$ there is no attractive interaction in our simulation. This result clearly demonstrates that phase A forms a network even when it is a minority phase. The process of the pattern formation shown in Fig. 9(c) is not compatible with droplet formation of phase B, but with network formation of phase A. The process of network formation resembles the network formation due to colloidal aggregation [23], and further viscoelastic phase separation of colloidal suspensions [34]. We emphasize that the wetting-

induced depletion attraction is stronger for the less volume fraction of phase A (see Fig. 8). This helps the formation of a network structure even for a small volume fraction of phase A.

V. SUMMARY

To summarize, we studied how wetting to particles affects a phase separation process of a binary fluid mixture. We found an unconventional attractive interaction between particles, which we call "wetting-induced depletion attraction." Inclusion of hydrodynamics leads to particle drift motion directly driven by "wetting-induced depletion attraction." This leads to an unusual reentrant morphological change as a function of the particle concentration. This interaction may be used to control the morphology of a binary mixture containing nanoparticles; for example, the formation of a particle network can be used for the formation of a conductive network of metallic particles. The relationship between wetting-induced network formation of particles and viscoelastic phase separation is also an interesting problem for future study.

Although our simulation is performed in 2D, its extension to 3D is straightforward. Although we expect the essential physics remains the same in 3D, this point should be checked carefully in the future.

ACKNOWLEDGMENT

This work was partially supported by a grant-in-aid from the Ministry of Education, Culture, Sports, Science and Technology, Japan.

[1] J. Israelachvili, *Intermolecular & Surface Forces* (Academic Press, London, 1985).
[2] J. W. Cahn, J. Chem. Phys. **66**, 3667 (1977); P. G. de Gennes, Rev. Mod. Phys. **57**, 827 (1985).
[3] S. Puri, J. Phys.: Condens. Matter **17**, R101 (2005).
[4] H. Tanaka, A. J. Lovinger, and D. D. Davis, Phys. Rev. Lett. **72**, 2581 (1994).
[5] H. Tanaka, J. Phys.: Condens. Matter **13**, 4637 (2001).
[6] B. P. Binks and J. H. Clint, Langmuir **18**, 1270 (2002).
[7] K. Stratford, R. Adhikari, I. Pagonabarraga, J.-C. Desplat, and M. E. Cates, Science **309**, 2198 (2005).
[8] H. Tanaka and T. Araki, Europhys. Lett. **51**, 154 (2000).
[9] A. Karim, J. F. Douglas, G. Nisato, D.-W. Liu, and E. J. Amis, Macromolecules **32**, 5917 (1999).
[10] H.-J. Chung, A. Taubert, R. D. Deshmunkh, and R. J. Composto, Europhys. Lett. **68**, 219 (2004).
[11] V. V. Ginzburg, F. Qiu, M. Paniconi, G. Peng, D. Jasnow, and A. C. Balaz, Phys. Rev. Lett. **82**, 4026 (1999).
[12] V. V. Ginzburg, G. Peng, F. Qiu, D. Jasnow, and A. C. Balaz, Phys. Rev. E **60**, 4352 (1999).
[13] A. C. Balaz, V. V. Ginzburg, F. Qiu, G. Peng, and D. Jasnow, J. Phys. Chem. B **104**, 3411 (2000).
[14] M. Laradji, J. Chem. Phys. **120**, 9330 (2004).
[15] F. Qiu, G. Peng, V. V. Ginzburg, A. C. Balaz, H.-Y. Chen, and D. Jasnow, J. Chem. Phys. **115**, 3779 (2001).
[16] D. Suppa, O. Kuksenok, A. C. Balaz, and J. M. Yeomans, J. Chem. Phys. **116**, 6305 (2002).
[17] R. Verberg, J. M. Yeomans, and A. C. Balazs, J. Chem. Phys. **123**, 224706 (2005).
[18] M. Laradji and G. MacNevin, J. Chem. Phys. **119**, 2275 (2003).
[19] Y. L. Tang and Y. Q. Ma, J. Chem. Phys. **116**, 7719 (2002).
[20] M. Laradji and M. J. A. Hore, J. Chem. Phys. **121**, 10641 (2004).
[21] A. Chakrabarti, J. Chem. Phys. **111**, 9418 (1999).
[22] B. P. Lee, J. F. Douglas, and S. C. Glotzer, Phys. Rev. E **60**, 5812 (1999).
[23] H. Tanaka and T. Araki, Phys. Rev. Lett. **85**, 1338 (2000); Chem. Eng. Sci. **61**, 2108 (2006).
[24] H. Kodama, K. Takeshita, T. Araki, and H. Tanaka, J. Phys.: Condens. Matter **16**, L115 (2004).
[25] T. Araki and H. Tanaka, J. Phys.: Condens. Matter **18**, L193 (2006).
[26] A. Onuki, *Phase Transition Dynamics* (Cambridge University Press, Cambridge, 2002).
[27] See, e.g., H. Furukawa, Phys. Rev. E **55**, 1150 (1997).
[28] V. Sofonea and K. R. Mecke, Eur. Phys. J. B **8**, 99 (1999).
[29] H. M. Tanaka, Prog. Theor. Phys. **101**, 863 (1999).
[30] A. J. Wagner and M. E. Cates, Europhys. Lett. **56**, 556 (2001).
[31] In 2D a network structure of phase A may be called a droplet structure of phase B. Since the domain shape of phase B is not relaxed by the interface tension to a spherical shape, we prefer to call it a network structure of phase A (see also the discussion on the dimensionality of a system in Sec. IV C).
[32] D. Beysens and D. Estève, Phys. Rev. Lett. **54**, 2123 (1985); R. R. Netz, *ibid.* **76**, 3646 (1996); C. Bauer, T. Bieker, and S. Dietrich, Phys. Rev. E **62**, 5324 (2000).
[33] R. Evans, U. Marini Bettolo Marconi, and P. Tarazona, J. Chem. Phys. **84**, 2376 (1986).
[34] H. Tanaka, Phys. Rev. E **59**, 6842 (1999); H. Tanaka, J. Phys.: Condens. Matter **12**, R207 (2000); H. Tanaka, Y. Nishikawa, and T. Koyama, *ibid.* **17**, L143 (2005).